

## MODELLING FOULING OF FLUTED HEAT TRANSFER SURFACES

P. Besevic<sup>1</sup>, S. M. Clarke<sup>2</sup> and D. I. Wilson<sup>1</sup>

<sup>1</sup> Department of Chemical Engineering and Biotechnology, New Museums Site, Pembroke Street, Cambridge, CB2 3RA, UK  
(email: diw11@cam.ac.uk)

<sup>2</sup> BP Institute and Department of Chemistry, Lensfield Road, Cambridge, CB2 1EW

### ABSTRACT

Enhanced heat transfer surfaces are frequently used in domestic and commercial heat transfer devices, including those used in heating, ventilation and air conditioning (HVAC) devices, including heat pumps. A simple analytical model was constructed to determine the effect of fluting geometry on heat transfer surface area and the impact of fouling. The performance of a fluted and a smooth tube were compared for a typical water heat pump application with condensing refrigerant as the hot utility. Deposition was assumed to give a uniform deposit thickness. Fouling affected the fluted and smooth tubes to differing extents. Whilst clean, the fluted tubes displayed significant heat transfer enhancement but this was more sensitive to deposition. As fouling increases, the extra area of the fluted geometry is offset by the increase in conduction length and the difference in performance of the two geometries becomes small. The results are generic: the intended application is in crystallisation fouling arising from hard water service. Fouling dynamics were not considered. The results establish the scope for further, detailed simulations.

### INTRODUCTION

Enhanced heat transfer devices are used where the volume of the device is important, such as in domestic, automobile and offshore applications. Many enhanced heat transfer devices employ complex geometries to increase the surface area available for heat transfer as well as creating fluid flow patterns which determine the amount of convective heat transfer (see Webb & Kim, 2005). Fouling can affect the performance of enhanced heat transfer systems by changing the surface area as well as introducing an unwanted conductive heat transfer resistance. The change in geometry will affect local heat transfer conditions, such as deposit interface temperatures, which are important in crystallisation and particulate fouling, so the change in internal geometry of the heat exchanger with respect to time should be considered in analyses of experimental data and predictions of device performance.

This paper considers the impact of fouling on a fluted tube geometry representative of the heat exchanger in a commercial heat pump system used for water heating. Heat

is provided by a refrigerant condensing in tubes arranged in a spiral around the fluted sections. Fluted tubes are formed by twisting or indenting a regular tube; spirally fluted tubes are sometimes referred to as spirally indented tubes. Reported tube side heat transfer enhancements over cylindrical tubes have exceeded 200% (Wang *et al.* 2000; Watkinson *et al.* 1974). There have been some experimental studies on the effect of fouling of spirally fluted tubes (*e.g.* Watkinson *et al.* (1974) and Watkinson & Martinez (1975) on scaling; Panchal (1989) on seawater biofouling). To the authors' knowledge, no modelling of the effect of fouling on spirally fluted tubes has been reported. Modelling of the performance of clean spirally fluted tubes has been undertaken (*e.g.* Rousseau *et al.* 2003), but these have not included the effect of fouling.

It is important to understand the effects of fouling and, in particular, thick deposit layers which can result from crystallisation fouling over prolonged periods. The application of interest is domestic heat pumps in hard water areas: these differ from those used in industrial applications insofar as long operating lifetimes are expected without any meaningful servicing. This is problematic when the process fluid has a high fouling tendency, such as hot water heaters in hard water areas. This paper presents a model that evaluates the effect of a growing fouling layer on the performance of a fluted heat transfer surface.

### CONFIGURATION

Figure 1 shows the simplified geometry used to represent the fluted tube. Refrigerant condenses in tubes coiled around the process duct. The curved wall is modelled as a series of toroids. Each of the toroidal cells, of length  $L$ , in Figure 1 will subsequently be referred to as a 'flute'.

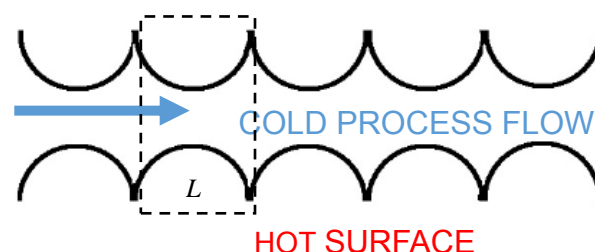


Fig. 1 Schematic illustrating the geometry of fluted pipe

Heat transfer in a fouled flute comprises contributions from condensing refrigerant, conduction through the walls and fouling layer, and forced convection in the process stream (water). Condensation is relatively fast and is assumed here to be insensitive to fouling (this can be modified if fouling affects nucleation involved in dropwise condensation). Heat transfer by conduction and convection are considered here. For flow in a smooth pipe, convective heat transfer can be modelled using the Dittus-Boelter equation and a similar empirical relationship is used as an estimator for a fluted pipe. Build-up of fouling material will modify the solid-liquid heat transfer area and the hydraulic diameter of the duct, both of which will change the rate of convective heat transfer. Similarly, the rate of heat transfer by conduction from the condensing fluid through the fouling layer is strongly related to the geometry of the system.

A long spirally fluted tube is modelled as series of fluted cells. The geometry is shown in detail in Figure 2.  $L$  is the flute pitch, or the length of a fluted cell. The radius of the flute is  $R$  and the position of a point on the wall can be described in terms of angle  $\theta$ .  $\theta_m$  is the maximum angle subtended for each flute until the next flute starts:  $0 \leq \theta_m \leq \pi/2$ , set by  $L$  and  $R$ . The duct through which the process stream flows is circular in cross-section when viewed along the tube axis, with radius  $r$  at a given axial location; this can be written as a function of  $\theta$ ,  $R$  and  $r_1$ , where  $r_1$  refers to the minimum radius of the clean pipe. Dimension  $r_2$  is the maximum radius of the process stream duct. The reference case is a smooth tube of radius  $r_c$ .

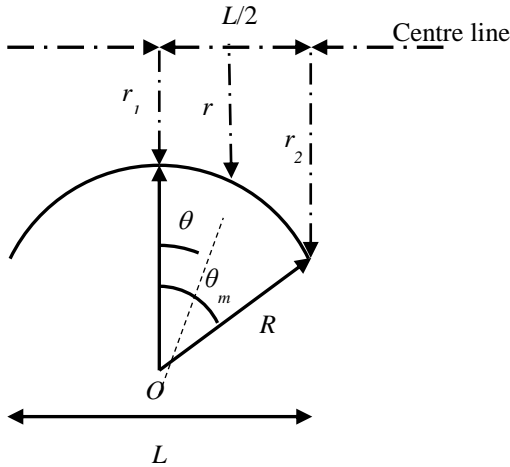


Fig 2. Schematic of a section through the wall illustrating key geometric features of a clean fluted cell.

**AREA ENHANCEMENT VIA FLUTING**

It can be shown that internal surface area of a clean single flute,  $A_{fl}$ , is given by

$$A_{fl} = 4 \pi R [(r_1 + R) \theta_m - R \sin \theta_m] \quad [1]$$

The area of a smooth tube of radius  $r_c$ ,  $A_s$ , is:

$$A_s = 2 \pi r_c L \quad [2]$$

where  $L$  is given by trigonometry as  $L = 2 R \sin \theta_m$ . The ratio of the areas of fluted and smooth pipes is:

$$\frac{A_{fl}}{A_s} = \frac{r_1}{r_c} \frac{\theta_m}{\sin \theta_m} - \frac{R}{r_c} \quad [3]$$

In order for the comparison in Equation (3) to be meaningful the diameters of the two geometries need to be comparable.

There is some disagreement in literature about the best way to estimate a diameter for a meaningful comparison between smooth and fluted tubes. In several experimental studies, authors have benchmarked the performance of fluted tubes against smooth pipes by comparing a smooth tube of equal diameter to the maximum diameter of the fluted tube (*i.e.*  $r_c \approx r_2$ , see Watkinson *et al.*, 1974). However, in one of the few modelling studies of clean fluted tubes, Rousseau *et al.*, (2003) employed a ‘volume based diameter’,  $d_v$ , defined as the diameter of a circular tube enclosing the same volume of fluid as a fluted tube for a given length, as below.

$$d_v = \sqrt{\frac{4V}{\pi L}} \quad [4]$$

where  $V$  is the volume of revolution swept out by rotating the wall in Figure 2 about the centreline.

It is reasonable to expect the ‘true’ hydraulic diameter of a fluted pipe lies between its maximum and minimum diameters. Given the lack of consensus in the literature, the arithmetic average of the the maximum and minimum radii of the duct is used here for the smooth tube in comparisons with a fluted tube:

$$r_c = \frac{r_1 + r_2}{2} \quad [5]$$

It is useful to express the radii in dimensionless terms based on the flute radius, for example

$$r_1^* = \frac{r_1}{R} \quad [6]$$

Figure 3 shows the effect of changing the duct diameter, *i.e.*  $r_1^*$ , on the ratio of areas for various values of  $\theta_m$ . The greatest enhancement in surface area is obtained with large  $\theta_m$ . As  $\theta_m$  decreases, the cross-section of the pipe appears flatter, and in the limiting case,  $\lim_{\theta_m \rightarrow 0} \frac{A_{fl}}{A_s} = 1$ , *i.e.*  $A_{fl} = A_s$ .

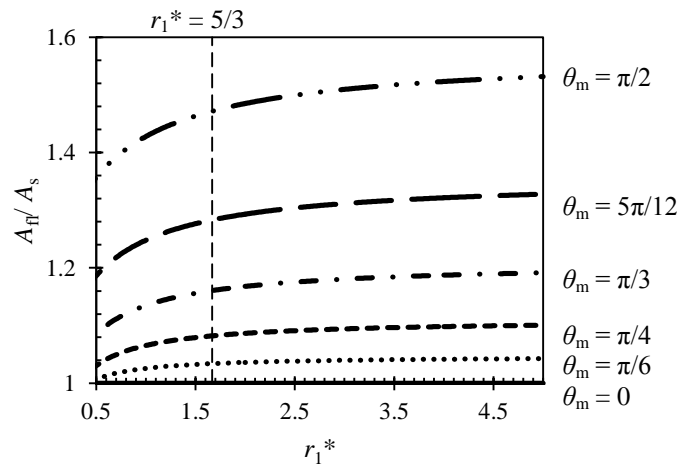


Fig. 3 Effect of flute dimensions on  $A_{fl} / A_s$ .

The Figure shows the area enhancement increases modestly with increasing  $r_1^*$  for  $r_1^* > 1$ . This result implies that many relatively small flutes give a greater increase in surface area than when the size of the flute is large relative to the radius of the tube. This is because the wall is further from the centre line of the tube, so a surface integral sweeps out a greater volume. In the limiting case, the size of the flutes are infinitesimally small and this is somewhat analogous to a surface made up of many small roughness elements. In the limiting case,  $\lim_{r_1^* \rightarrow \infty} \frac{A_{fl}}{A_s} = \theta_m \operatorname{cosec} \theta_m$ .

Figure 3 indicates that the area enhancement is strongly dependent on  $\theta_m$ . Figure 4 shows the effect of changing  $\theta_m$  for a fixed value of  $r_1^*$  for the case where  $r_1^* = 5/3$ , taken as a representative value for a heat pump heat exchanger. The enhancement is greater at high angles because more surface area is generated for small increments in pipe flute length.

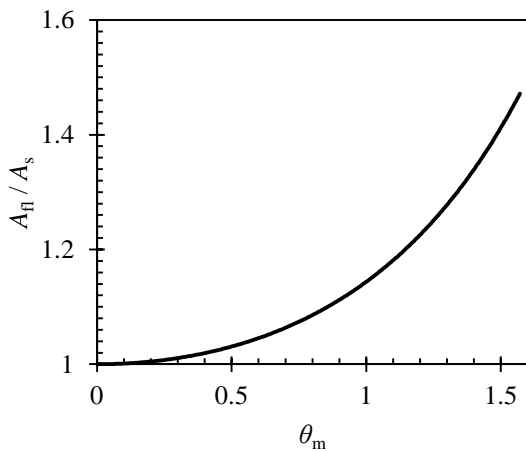


Fig. 4 Effect of  $\theta_m$  on  $A_{fl} / A_s$  for  $r_1^* = 5/3$ .

For clean devices, Figures 3 and 4 indicate that it is preferential to have many small flutes which subtend a large angle (large  $r_1^*$  and  $\theta_m$ ). This result can also be interpreted as suggesting that for a given size of flute, the area ratio can be increased by using a large diameter tube.

This conclusion, however, does not consider that area enhancement is used to reduce the volume or physical dimensions of a unit, particularly when space is at a premium. Consider the geometry of the unit in Figure 2; when fitted with the refrigerant coils, the total radius of the pipe, assuming the heating coils fit in the flutes, is  $r_1 + 2R$ . The volume of a unit of length  $L$ ,  $V_{HEX}$ , is  $\pi (r_1 + R)^2 L$ . Using Equation [1] for  $A_{fl}$  allows the heat transfer area per unit exchanger volume to be calculated. The plot of  $A_{fl} / V_{HEX}$  against  $r_1^*$  in Figure 5 shows that there is an optimal value of  $r_1^*$ , at around 1.26. If the unit was not subject to fouling, this would offer optimal performance in terms of compact heat transfer. The disadvantage associated with a slightly larger value of  $r_1^*$ , such as the value of  $5/3$  used in the calculations here, is however small as the  $A_{fl} / V_{HEX}$  ratios are similar. It will be shown in the next section that fouling reduces  $A_{fl}$  significantly: starting with a larger unit ( $r_1^* > 1.26$ ) will offer more resilience to fouling, albeit at the cost of a larger unit.

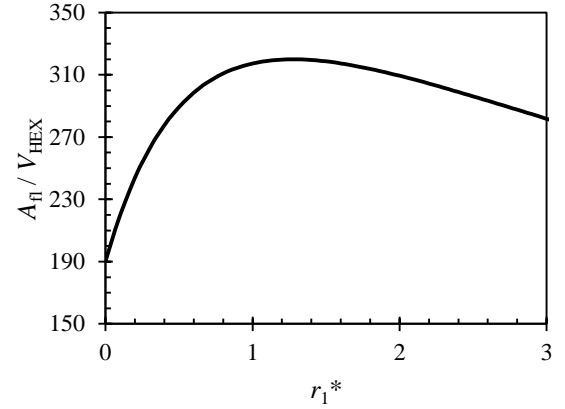


Fig. 5 Effect of  $r_1^*$  on surface area to unit volume,  $A_{fl} / V_{HEX}$ .

### EFFECT OF FOULING ON AREA ENHANCEMENT

The effect of buildup of a fouling layer on the heat transfer surface is now considered. Figure 6 shows a sketch of the fouled fluted system. The fouling layer is assumed to be isotropic and homogeneous, and the growth rate is the same in all directions. The fouling layer has thickness  $\delta$ . The maximum angle is now  $\theta_{mf}$ , which is related to  $L$ ,  $R$  and  $\delta$  via:

$$\sin \theta_{mf} = \frac{L}{2(R + \delta)} \quad [7]$$

It is also assumed that fouling layers on adjacent flutes grow at similar rates so that for adjacent flutes,  $\theta_{mf, \text{left}} \approx \theta_{mf, \text{right}}$  and the cells are symmetrical about  $\theta = 0$ . The cell can then be modelled using a half-cell as shown in the Figure.

The radius,  $r$ , of the duct for the process stream in the presence of a fouling layer is given by:

$$r = (r_1 + R - (R + \delta) \cos \theta) \quad [8]$$

A differential element of surface area for a fouled, fluted pipe,  $dA_{f, fl}$  is then

$$dA_{f, fl} = 2 \pi r (R + \delta) \cos(\theta) d\theta \quad [9]$$

The ratio of the thickness of the fouling layer to the size of a flute,  $\delta^*$ , is defined by

$$\delta^* = \frac{\delta}{R} \quad [10]$$

Integrating Equation (9) from  $0 \leq \theta \leq \theta_{mf}$  gives the area of the process stream-fouling layer interface,  $A_{fl, f}$ , as:

$$A_{fl, f} = 4\pi R^2 (1 + \delta^*) \left( (r_1^* + 1) \theta_{mf} - (1 + \delta^*) \sin(\theta_{mf}) \right) \quad [11]$$

The effect of deposition on the internal surface area for heat transfer is presented in Figure 6 for the case of a heat pump exchanger with dimensions  $R = 3$  mm,  $L = 6$  mm,  $r_1 = 5$  mm,  $r_2 = 8$  mm,  $\theta_m = \pi/2$ . The interfacial area is compared between fouled and clean fluted pipes. The result for a fouled, smooth tube, is also plotted: its area is

$$A_{s, f} = 4 \pi (r_c - \delta) R \sin \theta_m \quad [12]$$

Inspection of Equations [11 and 12] indicate that the reduction in surface area with respect fouling layer

thickness is non-linear with  $\delta^*$  for fluted pipes but linear for smooth ones. Moreover, the reduction in surface area is most sensitive at small fouling layer thicknesses.

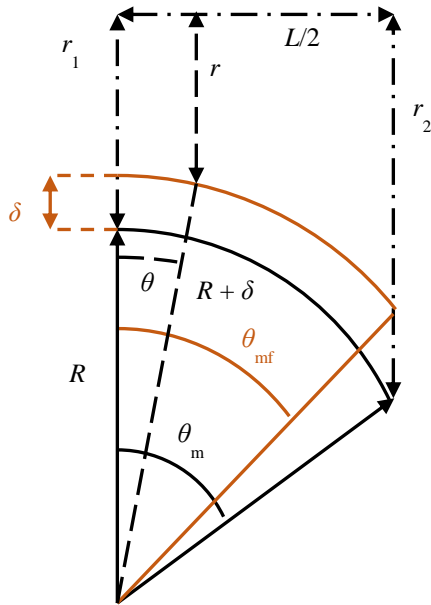


Fig. 6 Schematic of a fouled fluted half-cell

Figure 7 shows that the fluted tube is more sensitive to fouling in terms of area reduction than smooth tubes. The area enhancement obtained from fluting is lost as deposit builds up, and the fluted result approaches that of the smooth tube around  $\delta^* \sim 0.6$ . The gradient,  $d\left(\frac{A_{n,f}}{A_{n,c}}\right)/d\delta^*$ , converges to  $d\left(\frac{A_{s,f}}{A_{n,c}}\right)/d\delta^*$  as  $\delta^* \rightarrow \infty$ . The loci for fluted

and smooth tubes cross around  $\delta^* \sim 0.6$ ; this indicates that the arithmetic average for  $r_c$  may have overestimated the representative diameter for comparing fluted and smooth tubes. The Figure emphasises that the advantage in heat transfer conferred by fluting is nullified by fouling layer build-up. Further analysis confirms that for large diameter tubes, as the space between flutes is filled, the internal geometry of the fluted system soon resembles a smooth tube. It should be noted that the local fouling rate has been assumed to be uniform in this model: the spatial variation of surface temperature and shear stress require further analysis of fluid flow and heat transfer.

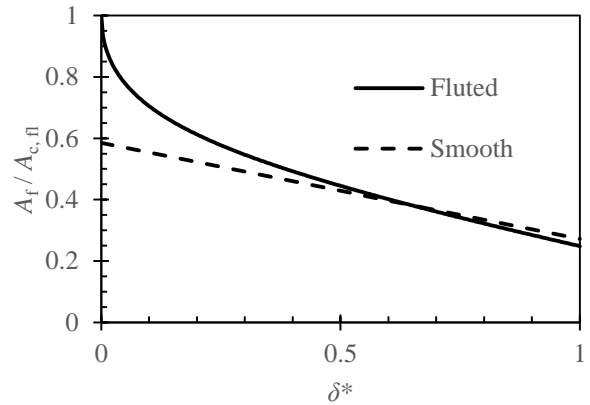


Fig. 7 Effect of fouling layer thickness on the ratio of fouled to clean heat transfer areas for a fluted and a smooth tube, for  $r_1^* = 5/3$ .

**EFFECT OF FOULING ON HEAT TRANSFER**

The model is now extended to consider heat transfer. Modelling of heat transfer through toroidal surfaces is complex and has seldom been attempted. Rousseau *et al.* (2003) reported numerical simulations of fluted tubes used

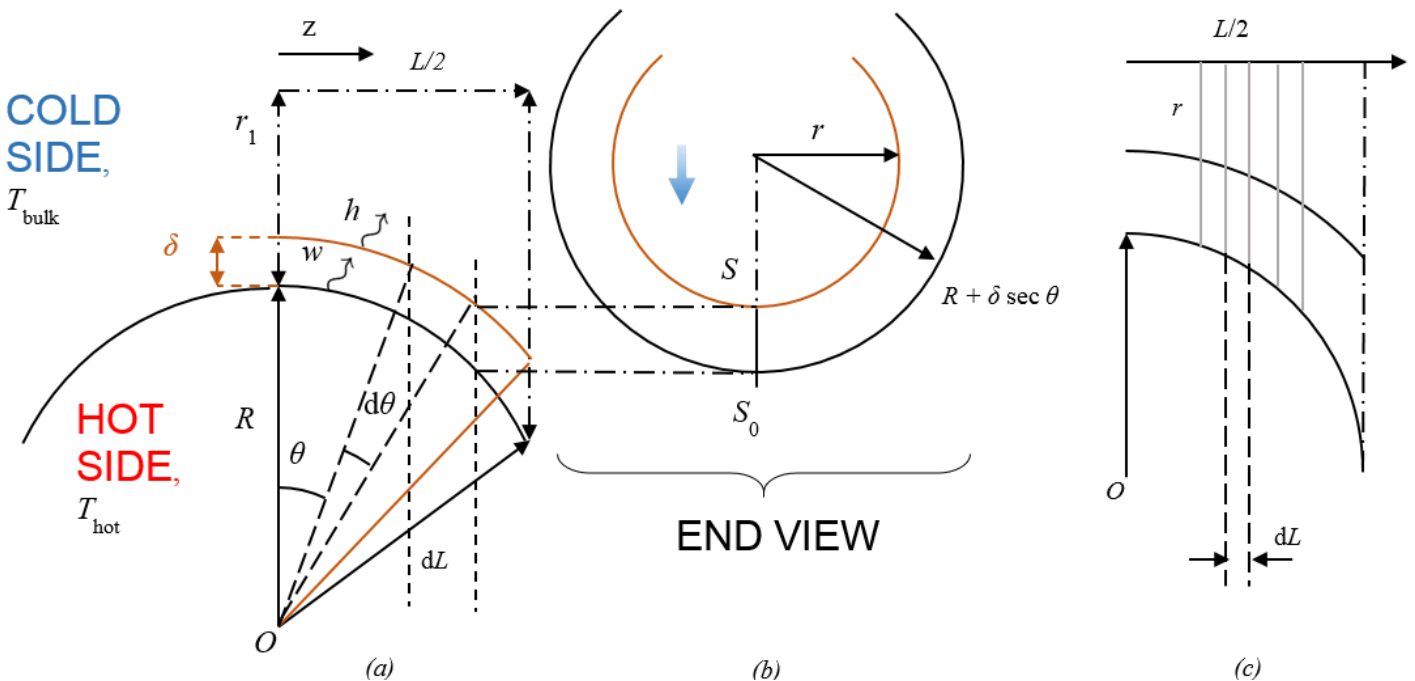


Fig. 8 Schematic of fouled flute geometry. (a) Slice through wall in pipe axis plane; (b) end view showing narrowing of flow cross-section as deposit layer grows; (c) Illustration of concentric annuli, for heat transfer calculations.

for water heating, but did not consider fouling.

Several underlying assumptions are made. Firstly, the heat source is a condensing fluid and so the external wall temperature,  $T_{\text{hot}}$ , is uniform. The wall is constructed from a high thermal conductivity metal so the external heat transfer coefficient,  $h_{\text{hot}}$ , is assumed to be uniform, finite and large. It is then assumed that the fouling layer changes both the film heat transfer coefficient,  $h_{\text{conv}}$ , and conduction through the deposit. The temperature driving force,  $\Delta T_{\text{overall}}$ , is defined as the difference between the condensing fluid temperature and the bulk temperature of the process fluid,  $T_{\text{bulk}}$ ;  $\Delta T_{\text{overall}} = T_{\text{hot}} - T_{\text{bulk}}$ . It is assumed that  $\Delta T_{\text{overall}}$  does not vary appreciably over one flute. Secondly, the unit is assumed to operate at constant throughput, with mass flow rate,  $\dot{m}$ .

Figure 8 summarises the geometrical features of heat transfer in the fouled state.  $S$  denotes the interface between the fouling layer and the process stream, while  $S_0$  refers to the clean surface. The fluted tube and fouling layer will be modelled as a series of differentially thin concentric annuli of thickness  $dL$  (Figure 8(c)). An individual slice is shown in end view, looking along the tube axis, in Figure 8(b). The local thickness of the fouling layer is given by  $\delta \sec \theta$ .

Firstly, consider conduction through the fouling layer in one of the differentially thin slices in Figure 7(c). The rate of heat transfer through the layer in the  $r$ -direction is given by

$$dQ = \frac{\lambda_f 2\pi(R+\delta) d\theta (T_{S_0} - T_s)}{\ln\left(\frac{r+\delta \sec \theta}{r}\right)} \quad [13]$$

where  $T_s$  is the temperature at  $S$ ,  $T_{S_0}$  is the temperature at  $S_0$ , and the thermal conductivity of the foulant is  $\lambda_f$ . This represents a simplification of the fully 3-dimensional case of conduction through a toroidal shell. It was deemed appropriate for this level of modelling.

$$\frac{dQ}{d\theta} = \frac{2\pi(T_{\text{hot}} - T_{\text{cold}})(R+\delta)}{\frac{1}{\lambda_f} \ln\left(\frac{(r_1+R-(R+\delta)\cos\theta)+\delta \sec \theta}{(r_1+R-(R+\delta)\cos\theta)}\right) + \frac{(R+\delta)\cos\theta - \delta \sec \theta}{(R+\delta)((r_1+R-(R+\delta)\cos\theta)+\delta \sec \theta)\cos\theta h_{\text{hot}}} + \frac{1}{b(r_1+R-(R+\delta)\cos\theta)^{-0.8}}}$$

The rate of convective heat transfer into the process stream at the fouling layer/process stream interface is given by:

$$dQ = 2\pi r (R+\delta) h_{\text{conv}} d\theta (T_s - T_{\text{bulk}}) \quad [14]$$

Finally, the rate of heat transfer from the heat source to the fouling layer/wall interface is estimated as

$$dQ = 2\pi(r+\delta \sec \theta) R h_{\text{hot}} d\theta^I (T_{\text{hot}} - T_{S_0}) \quad [15]$$

where  $h_{\text{hot}}$  is the heat transfer coefficient across the wall. Equation (15) contains a slightly different angular term,  $d\theta^I$ ;  $d\theta^I$  is used because the fouled surface and clean surface have differing radii, so for the thin axial slice as in Figure 7(c), the angles subtended by the clean and fouled surfaces differ.

$d\theta^I$  and  $d\theta$  are related thus:

$$d\theta^I = \frac{(R+\delta)^2 d\theta}{R((R+\delta)\cos\theta - \delta \sec \theta)} \quad [16]$$

Combining Equations (13 – 16) gives:

$$\frac{dQ}{d\theta} = \frac{2\pi(T_{\text{hot}} - T_{\text{cold}})(R+\delta)}{\frac{1}{\lambda_f} \ln\left(\frac{r+\delta \sec \theta}{r}\right) + \frac{(R+\delta)\cos\theta - \delta \sec \theta}{(R+\delta)(r+\delta \sec \theta)\cos\theta h_{\text{hot}}} + \frac{1}{r h_{\text{conv}}}} \quad [17]$$

The forced convection heat transfer coefficient will vary with axial position as the bulk velocity changes with position. The flow is turbulent, so detailed flow calculations would require 3-dimensional numerical simulations. It is therefore assumed that  $h_{\text{conv}}$  can be estimated using correlations for steady flow. For a fluted pipe, the Nusselt number can be estimated using the correlation based on experimental data presented by Panchal *et al.* (1992) and Park *et al.* (2013).

$$Nu_{\text{fluted}} = \frac{h_{\text{conv}} d_H}{k_{\text{water}}} = 0.071 \left(\frac{4\dot{m}}{\mu \pi d_H}\right)^{0.8} Pr^{0.4} \quad [18]$$

Inspection of Equation [18] indicates that the convective heat transfer coefficient scales with  $d_H^{-1.8}$ , where  $d_H$  is the hydraulic diameter. This relationship is assumed to hold for the fouled state (*i.e.* roughness effects are considered negligible) so that  $h_{\text{conv}}$  at radius,  $r$ , can be related to the clean coefficient,  $h_{\text{conv, clean}}$ , and the clean radius,  $r_{\text{clean}}$ , via

$$r h_{\text{conv}} = r_{\text{clean}}^{1.8} h_{\text{conv, clean}} r^{-0.8} \quad [19]$$

Writing  $r_{\text{clean}}^{1.8} h_{\text{conv, clean}}$  as a constant,  $b$ , yields

$$\frac{dQ}{d\theta} = \frac{2\pi(T_{\text{hot}} - T_{\text{cold}})(R+\delta)}{\frac{1}{\lambda_f} \ln\left(\frac{r+\delta \sec \theta}{r}\right) + \frac{(R+\delta)\cos\theta - \delta \sec \theta}{(R+\delta)(r+\delta \sec \theta)\cos\theta h_{\text{hot}}} + \frac{1}{b r^{-0.8}}} \quad [20]$$

Writing  $r$  as  $(r_1 + R - (R + \delta) \cos \theta)$  gives Equation (21), which is then integrated numerically between 0 and  $\theta_{\text{mf}}$  to give the rate of heat transfer for a single flute,  $Q$ .

A similar series of equations can be constructed for a smooth pipe for comparison with the fluted pipe. In this case  $b$  is replaced by constant  $c$ , obtained from the Dittus-

Boelter equation rather than Equation (18). [21]

The rate of heat transfer across one flute length for a clean, smooth tube is given by

$$Q_s = \frac{4\pi(T_{\text{hot}} - T_{\text{cold}})R \sin \theta_m}{\frac{1}{\lambda_f} \ln\left(\frac{r_c}{r_c - \delta}\right) + \frac{1}{r_c h_{\text{hot}}} + \frac{1}{c(r_c - \delta)^{-0.8}}} \quad [22]$$

## RESULTS AND DISCUSSION

### Predicted performance

Results are presented for a device with the geometry reported above, a water flow rate of 1 litre/min, and a log mean temperature difference (set as  $\Delta T_{\text{overall}}$  for one flute) of 50 K, which is representative of heat pumps in water heating service. The fouling layer was taken to be

crystalline calcium carbonate, with a thermal conductivity of 0.97 W/mK (after Pääkkönen *et al.*, 2015). The wall heat transfer coefficient,  $h_{\text{hot}}$ , was set as 5000 W/m<sup>2</sup> K, which is typical for condensation in a heat pump (Kim *et al.* 1992), and it taken to be insensitive to the extent of fouling. The flute geometry was defined using the same geometric terms as the fluted tube described in Figure 6,  $R = 3$  mm,  $L = 6$  mm,  $r_1 = 5$  mm,  $r_2 = 8$  mm,  $\theta_m = \pi/2$ .

A clean flute is more efficient at transferring heat than a cylindrical tube. The overall heat transfer coefficients were 4000 W/m<sup>2</sup> K and 1000 W/m<sup>2</sup> K for the fluted and straight tubes, respectively. The former value is similar in magnitude to the experimental value for clean fluted pipes reported by Watkinson *et al.* (1974).

Figure 9(a) shows the effect of fouling layer thickness on the rate of heat transfer in one flute for fluted and smooth tubes. At a fouling layer thickness corresponding to  $\delta^* \approx 1$ , the overall heat transfer coefficient of the fluted geometry has fallen to approximately 600 W/m<sup>2</sup> K, which is comparable to field measurements for fouled heat pump heat exchangers.

The sensitivity of the fluted tube performance seen in Figure 7 is even more pronounced in the heat transfer rate, indicating that enhancement is not simply a surface area effect. The performance of the fluted tube falls to 20% of the initial value by  $\delta^* = 0.2$ . The smooth tube performance also falls significantly over this range relative to its clean value. This result indicates that heat transfer is becoming dominated by conduction through the fouling layer. This is confirmed by the plots of fouling Biot number, defined as  $Bi_f = U_{\text{overall}} R_{f, \text{overall}}$ , in Figure 9(b).  $U_{\text{overall}}$  was calculated by using the heat transfer equation for each fluted cell,  $Q = U_{\text{overall}} A_{\text{fl}, f} \Delta T$ ; similarly, the fouling resistance,  $R_f$ , was calculated by  $R_f = \frac{1}{U_f} - \frac{1}{U_c}$ , where  $U_f$  represents the fouled overall heat transfer coefficient for the cell and  $U_c$  is the clean overall heat transfer coefficient. A fouling Biot number of zero corresponds to a clean surface, whereas a fouling Biot number of 4 indicates severe fouling (Esawy *et al.*, 2011). Figure 10(b) confirms that fluted tubes are more sensitive to fouling than smooth tubes.

The fact that the heat exchangers are so sensitive to fouling makes careful design choices and fouling mitigation strategies important. In both cases, at large  $\delta^*$  the performance of the fluted and smooth systems converge.

The validity of these predictions are now considered. Comparison with industrial data indicate that the heat transfer results are of the the correct order of magnitude (Kawaley, 2015). Figure 10 shows a photograph of a section taken through a fouled heat exchanger tube removed from a heat pump after some months of heating hard water. A thick layer of calcium carbonate scale is evident. The fouling layer thickness is about a third of the flute radius; fouling layers of greater thickness have been observed, so it is reasonable to plot values up to and including  $\delta^* \approx 1$ .

It can also be seen in Figure 10 from the flute cross sections that the flutes are not true circular arcs. The model geometry is therefore inexact.

The assumption that the convective heat transfer coefficient could be estimated using Equation (17) is unlikely to be valid in the initial stages of fouling. The body of fluid in the ‘valleys’ between flutes, *e.g.* between labels B and C, is likely to feature recirculation zones, giving long fluid recirculation times in these regions and promoting crystallisation. The assumption of uniform fouling rates would no longer hold. Incorporating these effects would require detailed fluid flow and thermal simulations.

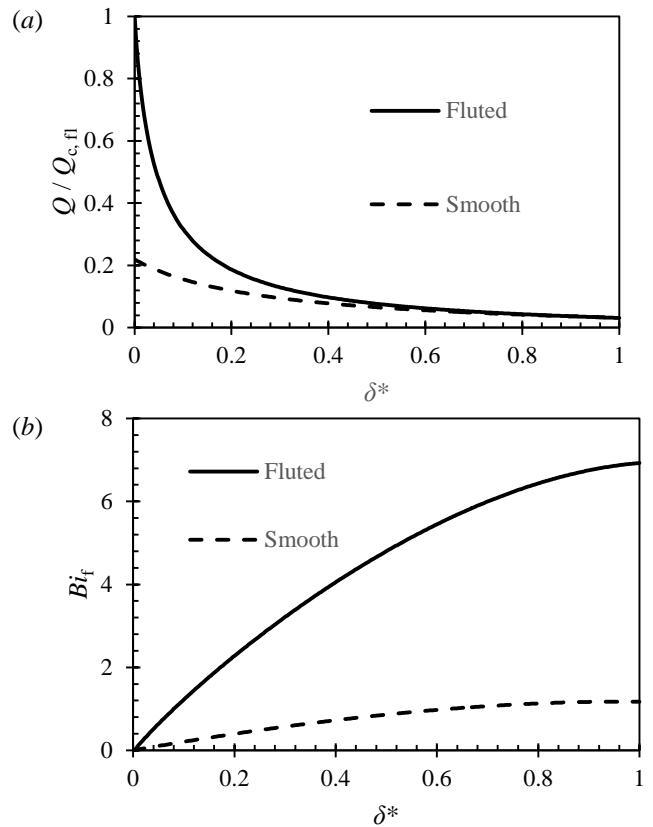


Fig. 9 Effect of fouling layer thickness on (a) the rate of heat transfer per flute, normalised by the rate of heat transfer in a single, clean flute; and (b) the fouling Biot number.

It is noticeable from the photograph that the fouling layers from the adjacent flutes merge at the midplane in the valleys, supporting the symmetry hypothesis employed in the analysis. Later on, when the layer thickness has reached that shown in the photograph, the analysis would appear to be reasonable:  $\theta_{mf}$  will have decreased to the extent that the valleys are excluded and do not make a significant contribution to heat transfer to the process stream.

Figure 9(a) suggests a 400% increase in heat transfer rate for a cleaned fluted pipe over that for a smooth pipe. Experimental studies by Watkinson *et al.* (1974) and Wang *et al.* (2000) suggested that spirally fluted heat transfer surfaces can provide a 200 % increase. Likely sources for this difference include (i) overestimation of the Nusselt number due to the inaccuracy of Equation (17) when

calculating  $h_{conv}$  at larger values of  $\theta$  (see the above discussion about valleys); (ii) overestimation of  $h_{hot}$ , as real units feature bonded components and there may be contact resistances present owing to imperfect welding in manufacturing; (iii) this model does not consider the effect of the angle of the fluting pitch (the condensing elements are spiral wound). This is reasonable for modelling at this level of scrutiny since experimental studies have not categorically determined any reproducible effect caused by this angle (Watkinson & Martinez, 1975).

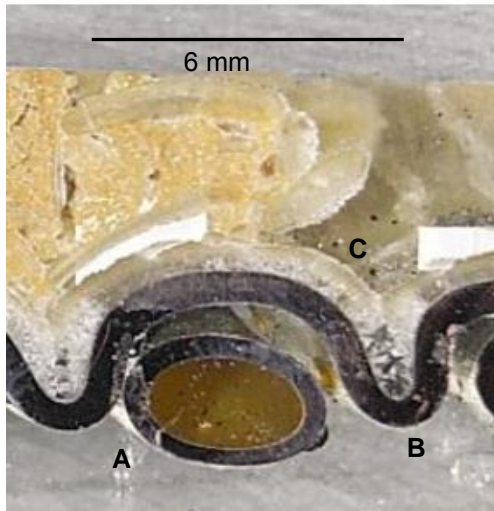


Fig. 10 Photograph of a section through the wall of a heat pump fluted tube exchanger in hard water service. A – refrigerant coil, B – fluted pipe wall, C – fouling layer.

**Sensitivity analysis**

The influence of the conduction resistance associated with the fouling layer is explored here by changing the thermal conductivity of the fouling layer. The geometrical features, including the change in fouling layer surface area and convective heat transfer coefficient, are then constant. Figure 11 shows that the initial decrease in the rate of heat transfer with increasing fouling layer thickness is very sensitive to the foulant thermal conductivity. This confirms that the conductive heat transfer terms in Equation 20 become more important as the fouling layer develops, and dominate the heat transfer behaviour of the system.

The thermal conductivity is likely to lie around 1 W/m K. The thermal conductivity of crystalline  $CaCO_3$  is around 5 W/m K but fouling layers formed on heat transfer surfaces are often porous and contain solution trapped in the voids (with a thermal conductivity close to that of water, at 0.6 W/m K). Experimental values range from 0.97 W/m K, reported by Pääkkönen *et al.* (2015), to 1.7-2.2 W/m K (Zhenhua *et al.*, 2008). Both lie within the above bounds. Ageing, as reported by Bohnet *et al.* (1999), is likely to increase  $\lambda_f$  at a rate determined by local temperature and diffusion conditions.

Figure 12(a) demonstrates that the process stream flow rate has little effect on the rate of heat transfer once the fouling layer is well established, *i.e.* at  $\delta^* \geq 0.1$ . A flow rate of 1 litre/min corresponds to a Reynolds number of about

2000. Conduction through the fouling layer again dominates the overall resistance to heat transfer. There is some sensitivity to flow rate at small  $\delta^*$ , shown in Figure 12(b). This Figure also demonstrates the rapid loss in performance of the fluted tube with a modest amount of deposit growth. Figure 7 indicates that the surface area for heat transfer has decreased by approximately 20% for  $\delta^* = 0.03$ : the additional loss in heat transfer performance arises from the resistance associated with conduction through the fouling layer.

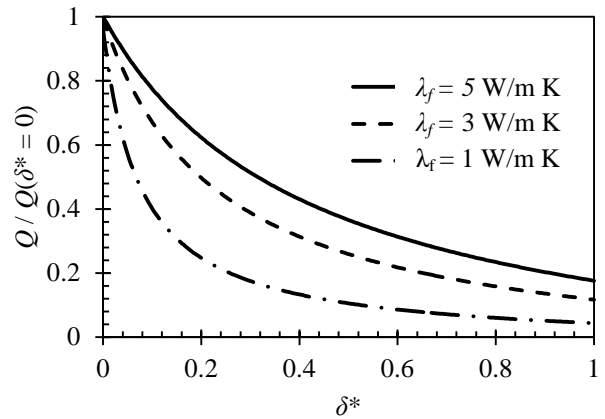
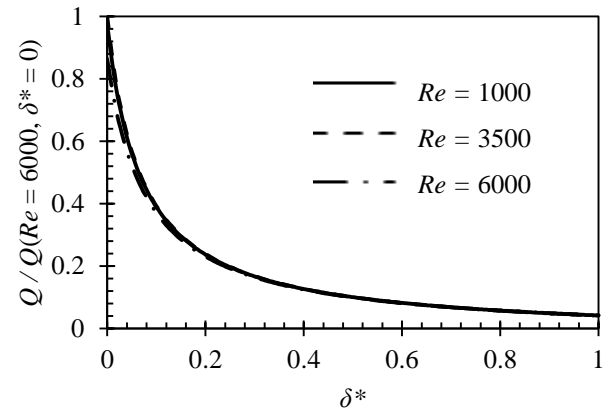


Fig. 11 Effect of fouling layer thickness for different foulant thermal conductivities

(a)



(b)

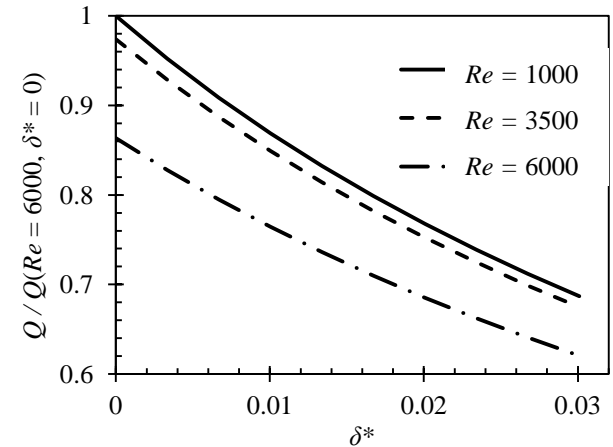


Fig. 12 Effect of process stream flow rate, expressed as Reynolds number, on rate of heat transfer. (a)  $\delta^* \leq 1$ ; (b) initial behaviour,  $\delta^* < 0.03$ ,  $\lambda_f = 0.97$  W/m K.

## Future Work

The model presented here does not incorporate all the features and physics of the real enhanced heat transfer tubes (shape of flutes, fluid flow patterns in flute valleys) but it demonstrates that the geometric features of fluted pipes make them more sensitive to fouling than smooth pipes. The model presently lacks fouling dynamics: these are currently being introduced using a crystallisation fouling model which includes local mass transport and temperature dependency.

Further dynamics associated with ageing are also under consideration as  $\lambda_f$  is likely to vary over time over the timescale required to deposit a thick layer of, for instance, calcium carbonate.

There are limitations to this modelling approach, particularly in relation to the description of the process stream fluid flow. Accurate quantification of the true flow pattern and thus the temperature distribution on the toroidal heat transfer surface would require 3-dimensional computational fluid dynamics simulations.

## CONCLUSIONS

A series of models were generated to quantify effect of fouling on fluted heat transfer surfaces relative to smooth ones. Clean fluted heat transfer surfaces gave significantly better heat transfer than smooth tubes, chiefly due to the higher surface area of the fluted tube, compared to a clean tube. As the fouling layer thickness increases, conduction through the fouling layer becomes important and eventually dominates the overall heat transfer coefficient. This is especially true for fluted tubes: large amounts of deposit effectively reduce fluted tube performance to that of a cylindrical tube with equivalent diameter. Fluted tubes may offer other engineering advantages over smooth tubes, for instance, it may be easier to attach heating coils or run a condensing medium over them, but for thick fouling layers, fluted surfaces do not optimise heat transfer performance relative to smooth surfaces.

## ACKNOWLEDGEMENTS

The authors gratefully acknowledge support from Mitsubishi Electric Corporation.

## NOMENCLATURE

$A_s, A_f$	area of smooth, fouled tube	$m^2$
$A_c$	area of clean tube	$m^2$
$A_{fl}$	area of fluted tube	$m^2$
$b$	constant	$W / m^{-0.2}$
$K$		
$Bi_f$	fouling Biot number	-
$c$	constant	$W / m^{-0.2}$
$K$		
$d_H$	hydraulic diameter	$m$
$d_v$	volume based diameter	$m$
$h_{conv}$	convective heat transfer coefficient	$W / m^2 K$
$h_{hot}$	hot side heat transfer coefficient	$W / m^2 K$
$k_{water}$	thermal conductivity of process fluid	$W / m K$
$L$	length of flute	$m$

$Q, Q_s$	heat transfer rate, smooth tube	$W$
$r$	flow channel radius	$m$
$r_1^*$	dimensionless flute radius	-
$r_1, r_2$	flow channel radius, minimum, maximum	$m$
$r_c$	radius of comparable smooth tube	$m$
$r_{clean}$	radius of clean tube	$m$
$R$	flute radius	$m$
$R_f$	fouling resistance	$m^2 K / W$
$T_{bulk}$	bulk fluid temperature	$^{\circ}C$
$T_{hot}$	hot side temperature	$^{\circ}C$
$T_s, T_{s0}$	temperature at surface, $S, S_0$	$^{\circ}C$
$U_c, U_f$	overall htc, clean, fouled	$W/m^2 K$
$V$	volume of flow channel	$m^3$
$V_{HEX}$	volume of assembled heat exchanger	$m^3$
$\delta$	fouling layer thickness	$m$
$\delta^*$	dimensionless fouling layer thickness	-
$\lambda_f$	thermal conductivity of fouling layer	$W / m K$
$\theta$	angle	-
$\theta_m, \theta_{mf}$	maximum angle, with fouling	-

## REFERENCES

- Bohnet, M., Augustin, W. and Hirsch, H., 1999, Influence of fouling layer shear strength on removal behaviour, in Bott, T.R., Melo, L.F., Panchal, C.B. and Somerscales, E.F.C (eds.) *Understanding Heat Exchanger Fouling & its Mitigation*, publ. Begell House, NY, 201-208.
- Esawy, M., Malayeri, M.R. and Müller-Steinhagen, H., 2011, Effect of deposit formation on the performance of annular finned tubes during nucleate pool boiling. In *Proc. Intl. Conf. on Heat Exchanger Fouling & Cleaning 2011*, Crete, pp. 119-125.
- Kawaley, G. 2015, Personal communication.
- Kim, T.S., Shin, J.Y., Chang, S.D., Kim, M.S., and Ro, S. 1992, Cycle performance and heat transfer characteristics of a heat pump using R22 / R142b refrigerant mixtures. In *Intl Refrigeration Air Conditioning Conference 1992*, Purdue
- Pääkkönen, T.M., Riihimäki, M., Simonson, C.J., Muurinen, E. and Keiski, R.L., 2015, Modeling CaCO<sub>3</sub> crystallization fouling on a heat exchanger surface – definition of fouling layer properties and model parameters. *Intl. J. Heat Mass Transfer*, Vol. 83, pp. 84-98.
- Panchal, C.B., 1989, Experimental investigation of sea water biofouling for enhanced surfaces, *Proc. ASME/AIChE National Heat Transfer Conference*, p26.
- Panchal, C.B., France, D.M. and Bell, K.J., 1992, Experimental investigation of single-phase, condensation, and flow boiling heat transfer for a spirally fluted tube, *Heat Transfer Eng*, Vol. 13, pp. 42-52.
- Park, H.J., Lee, D.H., and Ahn, S.W., 2013, Study of local heat transfer in a spirally fluted tube, *Intl. J. Thermal Sci*, Vol. 64, pp. 257-263.
- Rousseau, P.G., Van Eldik, M. and Greyvenstein, G.P., 2003, Detailed simulation of fluted tube water heating condensers. *Intl. J. Refrigeration*, Vol. 26, pp. 232-239.
- Wang, L., Sun, D.W., Liang, P., Zhuang, L. and Tan, Y., 2000, Heat transfer characteristics of carbon steel spirally fluted tube for high pressure preheaters, *Energy Conversion Management*, Vol. 41, pp. 993-1005.

Watkinson, A.P., Louis, L. and Brent, R., 1974, Scaling of enhanced heat transfer tubes, *Can. J. Chem. Eng.*, Vol, 52, pp. 558 – 562.

Watkinson, A. P. and Martinez, O., 1975, Scaling of spirally indented heat exchanger tubes, *J. Heat Transfer*, Vol. 97(3), pp. 490–492.

Zhenhua, Q. Yongchang C. and Chongfang, M.A., 2008, Experimental study of fouling on heat transfer surface during forced convective heat transfer, *Chinese J. Chem. Eng.*, Vol. 16(4), pp. 535-540.

Webb, R.L. and Kim, N.-H. (2005). *Principles of Enhanced Heat Transfer* publ. Taylor & Francis, Abingdon.